Neuron, Vol. 23, 569–582, July, 1999, Copyright ©1999 by Cell Press

Shank, a Novel Family of Postsynaptic Density Proteins that Binds to the NMDA Receptor/PSD-95/GKAP Complex and Cortactin

Scott Naisbitt,* Eunjoon Kim,§ Jian Cheng Tu,† Bo Xiao,† Carlo Sala,* Juli Valtschanoff,‡ Richard J. Weinberg,‡ Paul F. Worley,† and Morgan Sheng*‖

*Howard Hughes Medical Institute
Department of Neurobiology
Massachusetts General Hospital and
Harvard Medical School
Boston, Massachussetts 02114
†Department of Neuroscience
Johns Hopkins University School of Medicine
Baltimore, Maryland 21205
‡Department of Cell Biology and Anatomy
University of North Carolina at Chapel Hill
Chapel Hill, North Carolina 27599
§Department of Pharmacology
Pusan National University
Pusan 609-735
Korea

Summary

NMDA receptors are linked to intracellular cytoskeletal and signaling molecules via the PSD-95 protein complex. We report a novel family of postsynaptic density (PSD) proteins, termed Shank, that binds via its PDZ domain to the C terminus of PSD-95-associated protein GKAP. A ternary complex of Shank/GKAP/PSD-95 assembles in heterologous cells and can be coimmunoprecipitated from rat brain. Synaptic localization of Shank in neurons is inhibited by a GKAP splice variant that lacks the Shank-binding C terminus. In addition to its PDZ domain, Shank contains a proline-rich region that binds to cortactin and a SAM domain that mediates multimerization. Shank may function as a scaffold protein in the PSD, potentially cross-linking NMDA receptor/PSD-95 complexes and coupling them to regulators of the actin cytoskeleton.

Introduction

Excitatory synaptic transmission in the mammalian brain is primarily mediated by the neurotransmitter glutamate acting on postsynaptic ionotropic glutamate receptors (particularly NMDA and AMPA receptors). In addition, glutamate stimulates a subset of metabotropic glutamate receptors (particularly the group I metabotropic glutamate receptors mGluR1α and mGluR5) concentrated in the postsynaptic membrane. The molecular mechanisms that underlie the postsynaptic localization and signaling capabilities of these glutamate receptors have been intensely studied in recent years. An emerging theme is that the different classes of glutamate receptors (NMDA, AMPA, and group I metabotropic glutamate receptors) interact via their cytoplasmic tails with distinct intracellular anchoring/scaffold proteins (Sheng, 1997). The ionotropic receptors interact with specific PDZ domain proteins: NMDA receptors with the PSD-95/SAP90 family of proteins (reviewed in Sheng, 1996; Kornau et al., 1997; Ziff, 1997; Craven and Bredt, 1998) and AMPA receptors with GRIP/ABP/PICK1 (Dong et al., 1997; O'Brien et al., 1998; Srivastava et al., 1998; Wyszynski et al., 1998; Xia et al., 1999). On the other hand, mGluR1α and mGluR5 interact with the Homer/Vesl family of EVH domain proteins (Brakeman et al., 1997; Kato et al., 1998; Tu et al., 1998; Xiao et al., 1998). These specific interactions may play a role in the synaptic targeting and cytoskeletal attachment of glutamate receptors. Perhaps more importantly, these anchoring proteins are thought to link their respective transmembrane receptors physically and functionally to the appropriate intracellular signaling pathways. For instance, PSD-95 may link NMDA receptors to neuronal nitric oxide synthase and a ras GTPase-activating protein (reviewed in Craven and Bredt, 1998), and Homer appears to couple mGluRs to the IP3 receptor (Tu et al., 1998). Despite recent advances, much remains to be learned about the molecular composition and the physiological functions of the protein complexes associated with PSD-95, GRIP, and Homer. Moreover, the apparent segregation of the different classes of glutamate receptors into parallel protein interaction pathways raises the question of whether the PSD-95-, GRIP-, and Homer-associated complexes cross-talk with each other via downstream protein interactions that have yet to be uncovered.

The postsynaptic density (PSD) can be visualized as an ultrastructural thickening of the postsynaptic membrane that is characteristic of excitatory synapses. Among the glutamate receptor complexes discussed above, the NMDA receptor/PSD-95 complex is the one most tightly associated with the PSD. In biochemical preparations of the PSD, NMDA receptors and PSD-95 are highly enriched and resistant to extraction by Triton X-100 and sarkosyl detergents, while AMPA receptors/GRIP and mGluRs/Homer are relatively soluble (Cotman et al., 1974; Cohen et al., 1977; Wenthold et al., 1992, 1996; Kennedy, 1997; Allison et al., 1998; Xiao et al., 1998). It is possible that the components of the NMDA receptor/PSD-95 complex comprise the major constituents of the core PSD remaining after extraction with strong detergents (Kennedy, 1997). Because they are likely to play critical roles in the structural organization of the synapse and in the transduction of NMDA receptor signals, these core PSD proteins are important to define and study.

Recently, we and others have identified a family of proteins (termed GKAP, SAPAP, or DAP) that is highly concentrated in the PSD and that binds to the guanylate kinase (GK) domain of PSD-95 (Kim et al., 1997; Naisbitt et al., 1997; Satoh et al., 1997; Takeuchi et al., 1997). GKAP appears to be tightly associated with PSD-95; it can be immunoprecipitated from the brain in a complex with PSD-95 family proteins (Kim et al., 1997), and it is consistently colocalized with PSD-95 in neurons, even

‖To whom correspondence should be addressed (e-mail: sheng@helix.mgh.harvard.edu).

in the absence of associated NMDA receptors (Rao et al., 1998). The GKAP family of proteins contains at least four members and undergoes complex alternative splicing, but the physiological roles of these variants are unknown. To gain insight into GKAP function, we screened for binding partners of GKAP, hoping to extend the network of protein interactions emanating from NMDA receptors into the PSD. Here, we report the identification of a novel family of proteins (termed Shank) specifically enriched in the PSD of excitatory synapses. Shank contains multiple putative protein interaction domains, including ankyrin repeats, the SH3 domain, the PDZ domain, the proline-rich domain, and the SAM domain. We show that the PDZ domain of Shank mediates binding to the C terminus of GKAP and that this interaction is important in neurons for the synaptic localization of Shank. In addition, the SAM domain is responsible for multimerization of Shank, and the proline-rich region contains a specific binding site for cortactin, an actin cross-linking protein involved in regulation of the cortical actin cytoskeleton (Wu and Parsons, 1993; Huang et al., 1997). In the accompanying paper, we show that Shank also interacts specifically with Homer and group I metabotropic glutamate receptors (Tu et al., 1999 [this issue of *Neuron*]). Thus, the Shank family proteins may be key organizers of the PSD, linking together the PSD-95 and Homer-based complexes and allowing their interaction with modulators of the actin cytoskeleton.

Results

Isolation and Primary Structure of the Shank Family of Proteins

To identify additional components in the postsynaptic PSD-95/GKAP complex, we searched for GKAP-binding proteins by the yeast two-hybrid method. Using as bait the C-terminal 76 residues of GKAP1a (originally termed GKAP in Kim et al., 1997), we obtained multiple copies of six distinct cDNAs from a screen of approximately 1.5×10^6 rat and human brain clones. No other interacting clones were isolated. Sequence analysis revealed that all six cDNAs were derived from three closely related genes. Four of the six interacting cDNA clones were overlapping sequences from the same gene; the remaining clones (r9 and h10) represented two distinct but highly homologous polypeptides (Figure 1A). We named the three GKAP-interacting genes Shank1–3, for the presence of an SH3 domain and multiple ankyrin repeats in the encoded polypeptides; the generic term Shank will be used for the whole family. The complete coding sequences of Shank1 and Shank3 were obtained following conventional hybridization screening of rat brain cDNA libraries (see Figure 2). During the cloning and sequencing of these cDNAs, complex alternative splicing of Shank1 (and other Shank family members) was revealed, with some variants resulting in severely truncated proteins (E. K., S. N., and M. S., unpublished data). To prevent future confusion in nomenclature, we refer to the Shank1 and Shank3 splice variants presented in Figure 2 as Shank1a and Shank3a, respectively. Shank1a consists of 2088 residues, and Shank3a, 1740 residues (Figure 2).

Shank proteins share a common domain organization, consisting of seven ankyrin repeats near the N terminus, followed by an SH3 domain, a PDZ domain, a long proline-rich segment, and a SAM domain at the C terminus (Figure 1A). All these motifs are potentially involved in protein–protein interactions, suggesting a possible scaffold function for the multidomain Shank polypeptides. Shank1a and Shank3a proteins (37% identical to each other over their entire length) are approximately 40% identical to the cortactin-binding protein CortBP1 (Du et al., 1998) over the region extending from the PDZ domain, where CortBP1 begins, to the C terminus. A higher degree of identity is seen within the specified domains. CortBP1 does not contain the N-terminal ankyrin repeats or SH3 domains present in Shank1a and Shank3a, although it shares the PDZ, proline-rich, and SAM domains.

The C Terminus of GKAP Binds to the PDZ Domain of Shank

The PDZ domain is the only domain present in all interacting Shank clones isolated from the yeast two-hybrid screen (Figure 1A), suggesting that the Shank PDZ domain mediates interaction with the GKAP1a C-terminal bait construct. This was confirmed by deletion analysis in the yeast two-hybrid system; the isolated Shank1 PDZ domain was sufficient for binding to GKAP1a C-terminal residues 591–666 (Figure 1B). Furthermore, GKAP interaction is specific for the PDZ of Shank, since GKAP1a (residues 591–666) does not associate with the PDZ domains of PSD-95, Chapsyn-110/PSD-93, or CASK (Figure 1B; data not shown). Similarly, neither an N-terminal region of GKAP1a (residues 1–100) nor the Kv1.4 C-terminal tail could bind the Shank1 PDZ, even though these baits did interact, respectively, with the GK and PDZ domains of PSD-95 (Figure 1B). The PDZ domain is also responsible for the interaction of Shank2 and Shank3 with GKAP1a (data not shown; see Tu et al., 1999).

PDZ domains typically bind to the last several residues at the C terminus of interacting proteins. Indeed, we found that the last seven residues of GKAP1a (660–666; -PEAQTRL) interacted with Shank1 as effectively and as specifically as the initial bait GKAP1a (residues 591–666) (Figure 1B). To define in detail the C-terminal residues involved in Shank PDZ binding, we assayed point mutants in the last four amino acids of GKAP1a for binding to Shank1 in the yeast two-hybrid system (Figure 1C). This analysis revealed that the final three residues of GKAP are important for specific binding to Shank. At the 0 position (the last amino acid), the wild-type residue leucine was preferred, but a conservative substitution with valine was tolerated; an alanine substitution at the very C terminus abolished interaction. At the −1 position, a positively charged amino acid (arginine or lysine) was greatly preferred over a negative charge (aspartate). At the −2 position, either threonine or serine supported Shank binding, but an alanine mutation abolished it. Changes at the −3 position (Q→E or Q→A) did not affect GKAP1a interaction with Shank (Figure 1C). This mutational analysis, which is not comprehensive, suggests that the C-terminal sequence preferred by Shank's PDZ domain is -X-T/S-R/K-L* (where X is any amino acid, and the asterisk represents a stop codon).

A

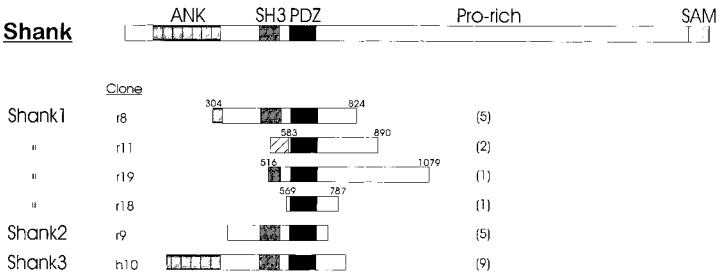

B

LexA \ GAD	Shank1(SH3-PDZ)	Shank1(PDZ)	PSD95(PDZ1-2)	PSD95(GK)
GKAP1a (591-666)	+++/+++	++/++	-/-	-/-
GKAP1a (660-666)	+++/+++	+++/+++	-/-	-/-
GKAP1a (1-100)	-/-	-/-	-/-	+++/+++
GKAP1b (602-627)	-/-	-/-	-/-	-/-
Kv1.4 (568-655)	-/-	-/-	+++/+++	-/-

C

	GKAP1a C-terminus				β-GAL/HIS3
(wt)	Q	T	R	L	+++/+++
	Q	T	R	V	+/++
	Q	T	R	A	-/-
	Q	T	K	L	++/+++
	Q	T	D	L	-/+
	Q	S	R	L	+/+++
	Q	A	R	L	-/-
	E	T	R	L	+++/+++
	A	T	R	L	+++/+++

Figure 1. The Domain Structure of Shank, and Interaction with GKAP1a

(A) Rat (r) and human (h) brain cDNA clones isolated from the yeast two-hybrid screen using GKAP1a C-terminal region (residues 591–666) as bait are shown aligned below a schematic of Shank protein (drawn to scale). Ank, Ankyrin repeats 1–7; SH3, Src homology 3 domain; PDZ, PSD-95/Dlg/ZO-1 domain; SAM, sterile alpha motif. Partial cDNAs from three related genes were isolated, termed Shank1, 2, and 3. Numbers in parentheses refer to the number of times each clone was isolated in the two-hybrid screen. Clone r11 contains an alternate N-terminal sequence (hatched) preceding the PDZ domain.

(B) The C terminus of GKAP1a interacts specifically with the PDZ domain of Shank. Interaction between GKAP1a (LexA fusions) and domains of Shank1 or PSD-95 (GAD fusions) were assayed by β-gal/HIS3 induction in the yeast two-hybrid system. The C-terminal seven residues of GKAP1a (660–666) are sufficient to bind the Shank1 PDZ domain but show no interaction with the PDZ domains of PSD-95. Neither GKAP1b C-terminal splice variant (residues 602–627, terminating GQSK) nor the Kv1.4 C-terminal (residues 568–655, positive control for the PDZ domains of PSD-95) can bind the PDZ domain of Shank1.

(C) Sequence requirements in the GKAP1a C terminus for interaction with Shank. The wild-type C-terminal sequence of GKAP1a (QTRL) is shown at top in bold. Single amino acid substitutions (bold, underlined) were introduced in the last four residues of GKAP1a (591–666). Interactions between mutant C termini and Shank1 (clone r8) were assayed as in (B).

Since all known members of the GKAP family (GKAP/SAPAP1–4) terminate with the same four amino acids (-QTRL) (Takeuchi et al., 1997), each member can presumably interact with Shank. However, it is noteworthy that splice variants of GKAP1 exist with alternative C termini, an example being GKAP1b (termed hGKAP in Kim et al., 1997). GKAP1b ends in the sequence GQSK* and does not interact with Shank (Figure 1B).

GKAP Binds Shank and Recruits Shank to PSD-95 Clusters in Heterologous Cells

To demonstrate biochemical association of GKAP and Shank proteins in a mammalian cell context, we performed coimmunoprecipitation from transfected COS7 cells (Figure 3A). Since GKAP is known to associate with PSD-95 (Kim et al., 1997), we included PSD-95 in these experiments. In cells triply transfected with wild-type GKAP1a + Shank1 + PSD-95, both GKAP and Shank could be coimmunoprecipitated by antibodies specific for either protein, but not by control (nonimmune IgG) antibodies (Figure 3A, lanes 1–4). GKAP antibodies also coprecipitated PSD-95, as expected. Antibodies to Shank brought down a significant amount of PSD-95 in addition to GKAP, implying the formation of a ternary complex containing Shank/GKAP/PSD-95 (Figure 3A, lane 3). We reasoned that a C-terminal point mutation in GKAP1a (changing the last amino acid L666→A) would abolish interaction with Shank but not interfere with binding to PSD-95, which is mediated by the N-terminal region of GKAP (Kim et al., 1997). In cells triply transfected with mutant GKAP1a(L666A) + Shank1 + PSD-95, Shank was not coprecipitated by GKAP antibodies, even though the cognate antigen GKAP was efficiently brought down (Figure 3A, lane 8). Moreover, PSD-95 was not significantly coprecipitated with Shank antibodies, though its coimmunoprecipitation with GKAP remained robust (Figure 3A, compare lanes 7 and 8). This experiment demonstrates that GKAP1a and Shank1 can associate in heterologous cells via a mechanism dependent on the C terminus of GKAP1a. Furthermore, GKAP1a can mediate the association of PSD-95 with Shank1. These findings are consistent with the formation of a ternary complex in which GKAP uses its N-terminal region to bind to PSD-95 and its C terminus to bind to Shank. Shank1 and GKAP1a also coimmunoprecipitate in the absence of PSD-95 (data not shown).

We have previously shown that PSD-95 and its relatives can cause the clustering of Shaker K^+ channels and NMDA receptors when coexpressed in COS7 cells (Kim et al., 1995, 1996) and that GKAP can be recruited into these clusters by binding to PSD-95 (Kim et al., 1997). To test whether GKAP might recruit Shank to PSD-95 clusters, we looked for coclustering in COS7 cells triply transfected with Shank1 + PSD-95 + GKAP1a or with Shank1 + PSD-95 + GKAP1b (the GKAP splice variant terminating in -GQSK* instead of -QTRL*)

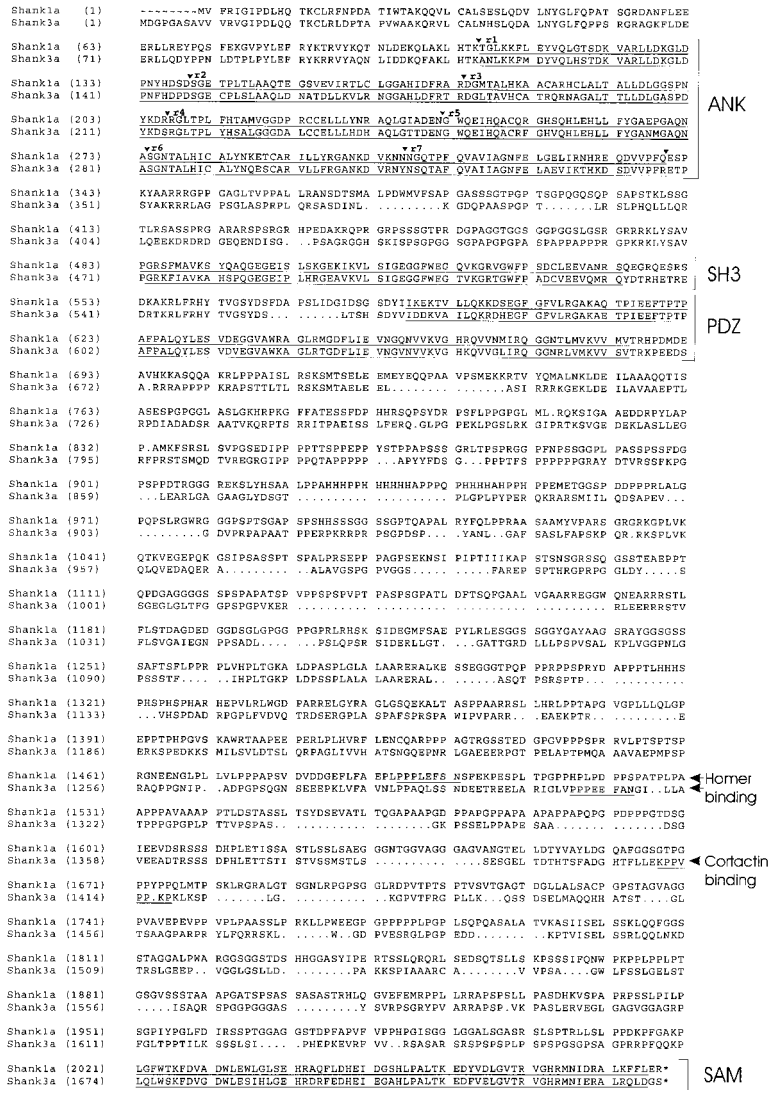

Figure 2. Amino Acid Sequence Alignment of Shank1a and Shank3a

Sequence begins at the most likely translation start site based on Kozak consensus. Domains are underlined and labeled as in Figure 1A. Ankyrin repeats (r1–r7) are separated by black wedges. The Homer EVH–binding motif (see Tu et al., 1999) and cortactin SH3-binding motif are also underlined.

(Figures 3B and 3C). When expressed individually, Shank1, PSD-95, and GKAP1 are distributed typically in a diffuse cytoplasmic pattern in COS7 cells (data not shown). Shank1 and PSD-95 do not directly interact, and as expected, these two proteins do not cluster together when coexpressed (data not shown). In contrast, cells triply transfected with Shank1 + PSD-95 + GKAP1a formed plaque-like clusters in which Shank immunoreactivity colocalized precisely with PSD-95 (Figure 3B) and with GKAP (data not shown). These clusters have an appearance identical to PSD-95/Shaker K^+ channel coclusters or NMDA receptor/PSD-95 coclusters (Kim et al., 1995, 1996). In cells transfected with Shank1 + PSD-95 + GKAP1b, however, Shank immunoreactivity remains diffuse and does not colocalize with PSD-95 (Figure 3C). PSD-95 and GKAP form coaggregates in these cells (Figure 3C, right), as they do even in the absence of Shank (data not shown). Thus, GKAP1a, but not GKAP1b, can mediate the coclustering of Shank1 with PSD-95 in heterologous cells. This is consistent with GKAP1a recruiting Shank1 via its specific C-terminal PDZ-binding sequence. Shank1 and GKAP1a do not form clusters in the absence of PSD-95 (data not shown). In summary, Shank1 can form coclusters with PSD-95 only in the presence of a GKAP splice variant that binds to Shank as well as to PSD-95. The GKAP1a-dependent coclustering of Shank1 and PSD-95 corroborates the coimmunoprecipitation results, indicating the formation in heterologous cells of a ternary complex of Shank/GKAP/PSD-95 that is specified by the C-terminal sequence of GKAP.

Association of Shank with the GKAP/PSD-95 Complex In Vivo

GST pulldown experiments from rat brain extracts were performed to verify biochemical association of Shank and GKAP. Sepharose beads charged with GST fusion protein of Shank1(SH3–PDZ) precipitated a large fraction of GKAP present in the offered extract (Figure 4A). In addition to GKAP, GST–Shank1(SH3–PDZ) brought down PSD-95, chapsyn-110/PSD-93, and NR1 (a subunit of NMDA receptors). These pulldowns were specific, since SAP97, synaptophysin, and glutamic acid

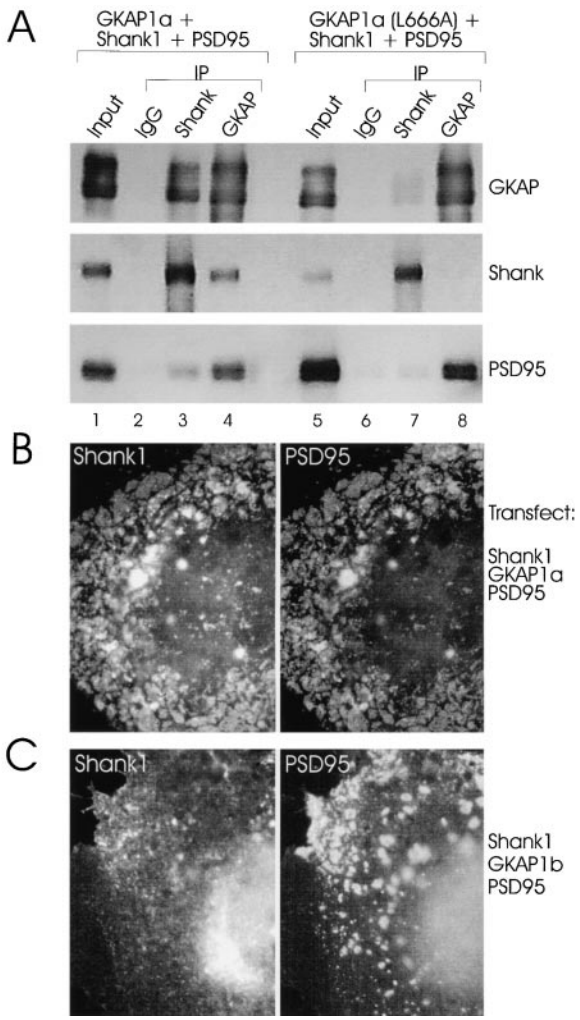

Figure 3. Coimmunoprecipitation and Coclustering of Shank, GKAP, and PSD-95 in Transfected COS7 Cells

(A) Extracts from COS7 cells triply transfected with wild-type GKAP1a + Shank1 + PSD-95 (lanes 1–4), or with GKAP1a mutant (L666A) + Shank1 + PSD-95 (lanes 5–8), were immunoprecipitated with Shank, GKAP, or control (nonimmune IgG) antibodies. The immunoprecipitates were immunoblotted for GKAP, Shank, and PSD-95, as indicated. Input lane was loaded with 10% of extract used for IP.

(B and C) COS7 cells were triply transfected with (B) GKAP1a + Shank1 + PSD-95 or (C) GKAP C-terminal splice variant GKAP1b + Shank1 + PSD-95. Cells were double labeled for Shank1 (Cy3, left panels) and PSD-95 (FITC, right panels). Shank coclusters with PSD-95 when cotransfected with GKAP1a (terminating QTRL*), but not when cotransfected with GKAP1b (terminating GQSK*). PSD-95 and GKAP form aggregates in these cells ([C], right) similar to those in Shank-untransfected cells (data not shown). Shank1 and PSD-95 do not cluster in the absence of GKAP (data not shown).

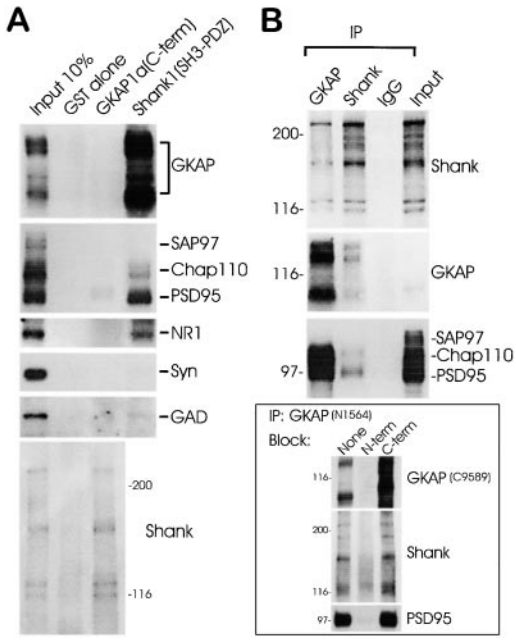

Figure 4. Biochemical Association of Shank, GKAP, and PSD-95 in Rat Brain

(A) GST pulldown assays showing GKAP–Shank binding. Beads charged with GST alone or GST fusions of GKAP1a (C-terminal residues 591–666) or Shank1(SH3–PDZ) (residues 469–691) were incubated with whole rat brain extracts. Bound proteins were immunoblotted for the indicated proteins. Input lane was loaded with 10% of the extract used for pulldown. The GST–Shank(SH3–PDZ) pulldown was not loaded for the Shank immunoblot because the antibody recognizes the GST–Shank fusion protein.

(B) Coimmunoprecipitation of Shank, GKAP, and PSD-95 from brain. Extracts of rat forebrain synaptosomal membranes were immunoprecipitated with GKAP, Shank, or control (nonimmune IgG) antibodies, as indicated. Immunoprecipitates were immunoblotted for Shank, GKAP, and the PSD-95 family of proteins. Input lane was loaded with 100% (top, Shank), or 10% (bottom, GKAP and PSD-95) of extract used for immunoprecipation. Inset, Specific block of immunoprecipitation by antigen. GKAP antibodies raised against the N-terminal region of GKAP (N1564) were used for immunoprecipitation of brain extracts. Immunoprecipitation of GKAP and coimmunoprecipitation of Shank and PSD-95 by N1564 were blocked by a thioredoxin fusion protein of the N-terminal region of GKAP (the antigen used to generate N1564), but not by a fusion protein of the C-terminal region of GKAP. Immunoblotting for GKAP was performed with antibodies directed against the C-terminal region of GKAP (C9589).

decarboxylase (GAD) were not precipitated with GST–Shank1(SH3–PDZ), and GST alone pulled down none of these proteins (Figure 4A).

In parallel, a GST fusion protein incorporating the C-terminal 76 amino acids of GKAP1a [GKAP1a(C-term)] specifically pulled down Shank proteins from brain extract (Figure 4A, bottom panel). Note that multiple Shank bands are seen on immunoblots of the brain. The specificity of these Shank bands is supported by two pieces of evidence: first, these signals are abolished upon preincubation of antibodies with Shank immunogen, and second, two additional antibodies raised against independent regions of Shank yield essentially identical immunoblot patterns (E. K., S. N., and M. S., unpublished data). The heterogeneity of Shank bands arises because our antibodies recognize multiple members of the Shank family and because each of the Shank genes undergoes complex alternative splicing (E. K., S. N., and M. S., unpublished data). Although the GKAP1a(C-term) fusion protein pulled down Shank, it did not pull down GKAP (Figure 4A). This is presumably because GST-GKAP1a(C-term) can only bind to Shank with an unoccupied

PDZ domain and, hence, will not bind to Shank proteins already complexed with native GKAP in the brain extract. Consistent with such an interpretation, GST-GKAP1a(C-term) can bring down Homer protein, which binds to Shank at a site distinct from the PDZ domain (see Tu et al., 1999). In summary, these pulldown results confirm the specific binding between GKAP and native Shank; furthermore, they indicate that Shank can bind to a native complex containing GKAP/PSD-95 and associated NMDA receptors.

To show that a ternary complex of Shank/GKAP/PSD-95 exists in vivo, we performed coimmunoprecipitations from solubilized synaptosomal membranes (Figure 4B). Shank antibodies immunoprecipitated Shank proteins with high efficiency, and in addition they coprecipitated significant amounts of GKAP and PSD-95 and chapsyn-110/PSD-93. Since Shank does not interact directly with PSD-95 family proteins, this result is consistent with Shank existing in a ternary complex with GKAP/PSD-95. Similarly, GKAP antibodies immunoprecipitated a large fraction of GKAP from the extracts, along with Shank, PSD-95, and chapsyn-110 (Figure 4B). Although this latter result does not prove the existence of the ternary complex, it does confirm the native association of GKAP with Shank and of GKAP with PSD-95 in the brain. None of the examined proteins was detectable in control IgG precipitates, indicating the specificity of the coimmunoprecipitations. Additionally, it is significant that SAP97 (a PSD-95 family protein; Müller et al., 1995) was not brought down with GKAP in either GST pulldown or antibody precipitation assays (Figures 4A and 4B), even though SAP97 has intrinsic binding affinity for GKAP (Kim et al., 1997). PSD-95 and chapsyn-110 cofractionate with GKAP as core components of the PSD, whereas SAP97 is segregated from GKAP in presynaptic and axonal compartments (Müller et al., 1995; Kim et al., 1996). The fact that GKAP and SAP97 do not coprecipitate thus offers reassurance that the detected protein–protein interactions are specific and not occurring artifactually after solubilization of the proteins. As a further test of specificity, we showed that the coimmunoprecipitation of Shank and GKAP could be blocked by competition with the specific antigen (Figure 4, inset). GKAP antibodies raised against the N-terminal region of GKAP (termed N1564) immunoprecipitated GKAP and coprecipitated Shank and PSD-95 in the absence of any blocking antigens. The precipitation of GKAP and the coprecipitation of Shank and PSD-95 by N1564 antibodies were blocked by preincubation with the N-terminal GKAP fusion protein antigen but not by a fusion protein of the C-terminal region of GKAP (Figure 4, inset).

Synaptic Localization of Shank in Cultured Neurons

The experiments above indicate the biochemical association of Shank, GKAP, and PSD-95 in the brain. Are Shank proteins also specifically localized at synaptic sites, like GKAP and PSD-95? This question was addressed by double-labeled immunofluorescence staining of cultured hippocampal neurons (Figure 5). The pattern of Shank immunoreactivity was strikingly punctate and distributed along dendrites of neurons. The punctate Shank staining matched closely that of synaptophysin, GKAP, PSD-95, and NR1, indicating the specific concentration of Shank in synapses (Figures 5A–5D). On the other hand, Shank-immunoreactive puncta showed no colocalization with the GABAergic synaptic marker GAD (Figure 5E), indicating Shank's absence from inhibitory synapses. Thus, at the light microscopy level, Shank is a synaptic protein found specifically in excitatory synapses, consistent with its interaction with the NMDA receptor/PSD-95/GKAP complex.

Biochemical and Electron Microscopic Evidence that Shank Is a Component of the PSD

To determine if Shank is a component of the PSD in vivo, we studied the fractionation of Shank proteins during biochemical purification of rat brain PSDs (Figure 6A). The heterogeneous set of Shank polypeptides was highly enriched in PSD preparations and was resistant to extraction by Triton X-100 and sarkosyl detergents. In fact, Shank enrichment during purification and detergent extraction of PSDs was similar to that of PSD-95 and GKAP (Figure 6A). The finding that Shank is a core component of the PSD provides further evidence that Shank is an authentic component of the NMDA receptor/PSD-95/GKAP complex.

Finally, we employed postembedding immunoelectron microscopy to investigate the subcellular location of Shank proteins in native brain tissue. Immunogold labeling for Shank in rat cerebral cortex is predominantly synaptic and associated with both axospinous and axodendritic asymmetric synapses. Most of the labeling is over the PSD, close to the postsynaptic membrane (Figure 6B). Quantitative analysis confirmed that Shank is concentrated on the postsynaptic side of the synapse; the peak of the distribution profile of Shank immunogold particles was approximately 25 nm inside the postsynaptic membrane (Figure 6C). Shank was relatively evenly distributed in the lateral plane of the synapse. These ultrastructural studies support the light microscopic and biochemical findings, confirming at high resolution that Shank is specifically concentrated in the PSD of excitatory synapses.

The GKAP–Shank Interaction Is Required for Shank Localization in Synapses

GKAP1b is a naturally occurring C-terminal splice variant of GKAP1 that binds to PSD-95 but not to Shank (see above). Unlike GKAP1a, GKAP1b is unable to recruit Shank into PSD-95 clusters in heterologous cells (see Figures 3B and 3C). We exploited these two GKAP isoforms to explore the in vivo significance of the GKAP–Shank interaction. Overexpression of GKAP1a (the Shank-binding isoform) in cultured hippocampal neurons caused an increase in the density of Shank immunoreactive clusters (93 $\pm$ 16 clusters per 100 μm dendrite versus 69 $\pm$ 9 in untransfected neurons) that did not reach statistical significance ($p = 0.22$; Figures 8Aa and 8Ae). By contrast, overexpression of GKAP1b caused a marked and significant ($p < 0.01$) decrease in synaptic clusters of Shank (to only 31 $\pm$ 4 puncta per 100 μm dendrite) (Figures 8Ab and 8Ae). The number of synaptic PSD-95 clusters was not affected ($p = 0.52$) by either GKAP1a or GKAP1b overexpression (Figures 8Ac, 8Ad, and 8Ae). Similarly, the density of synaptophysin puncta was not significantly altered (data not shown; $p = 0.35$). These findings indicate that the GKAP1a C

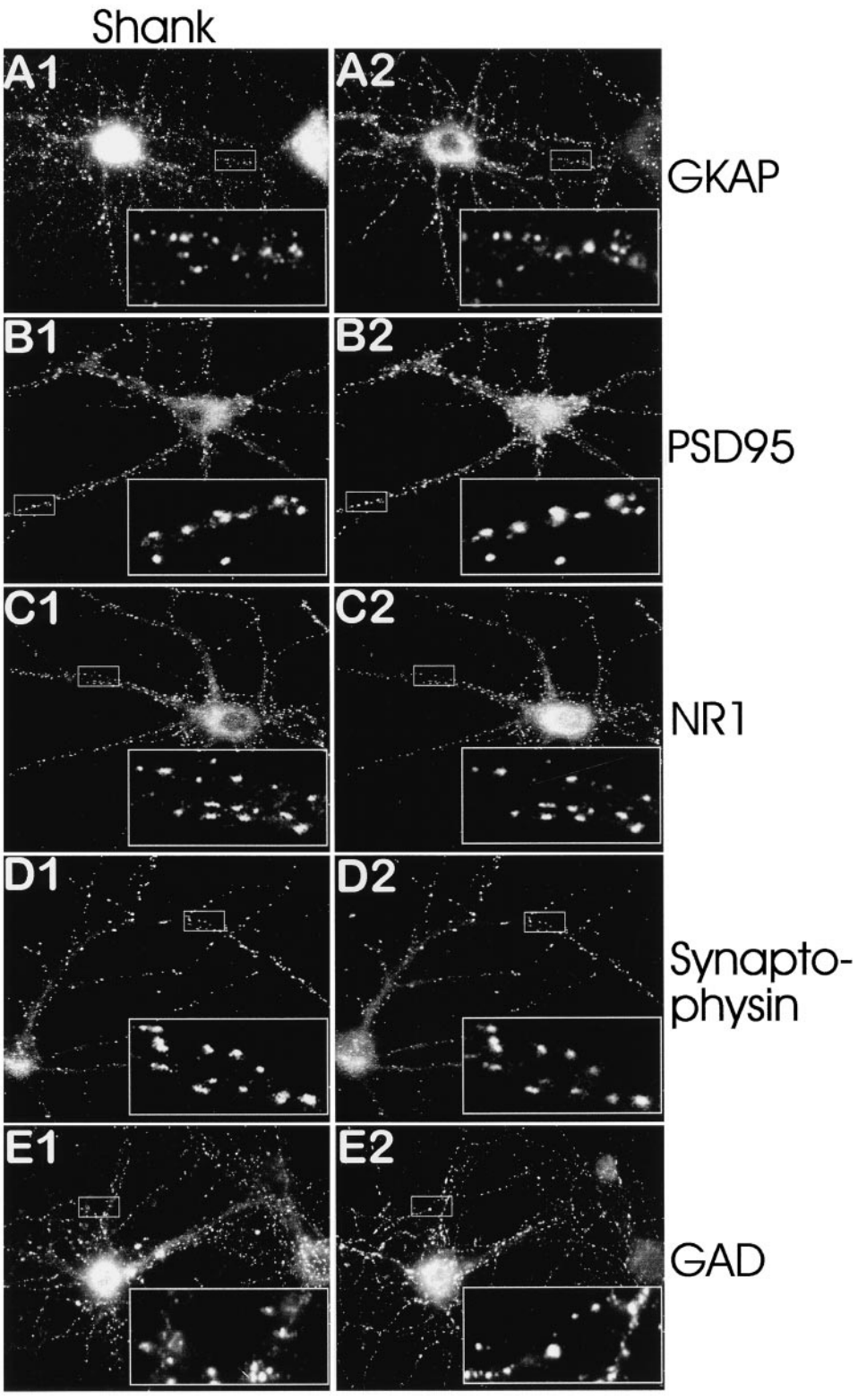

Figure 5. Localization of Shank at Excitatory Synapses in Cultured Hippocampal Neurons

Hippocampal neurons at 2–3 weeks in vitro were double labeled for Shank (left column, A1 to E1) and various proteins as indicated (right column, A2 to E2). Shank colocalizes in a punctate pattern with GKAP, PSD-95, NR1, and synaptophysin, but not with GAD. Enlargements of the indicated rectangular fields are shown in insets at bottom right of each panel.

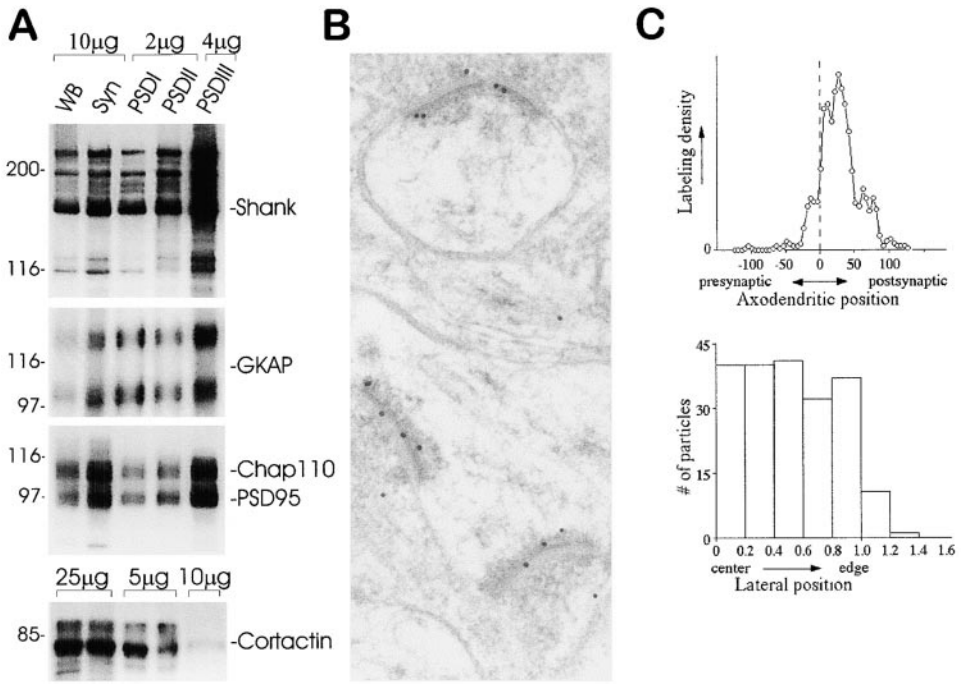

Figure 6. Biochemical Enrichment and Quantitative Immunogold Electron Microscropic Localization of Shank in PSD

(A) Immunoblot analysis of brain and PSD fractions (amount of protein loaded in each lane is indicated). WB, Whole brain homogenate; Syn, crude synaptosomes; PSD fractions were extracted with Triton X-100 once (PSDI), twice (PSDII), or with Triton X-100 followed by sarkosyl (PSDIII). Blots were probed for the indicated proteins, showing enrichment in PSD of Shank similar to that of GKAP, PSD-95, and chapsyn-110. Cortactin is enriched in PSDI but not PSDIII.

(B) Postembedding immunogold EM labeling of Shank in a representative section from adult rat cerebral cortex, showing Shank labeling predominantly over the PSD of asymmetric synapses.

(C) Quantitative analysis of the distribution of Shank immunogold particles at synapses. Fields containing Shank immunopositive synapses were digitized, and all gold particles within 150 nm of an active zone were analyzed. The distance of immunogold particles from the inner leaflet of the postsynaptic membrane in the axodendritic axis is plotted in the upper panel (in nm; 0 represents postsynaptic membrane). The distance of gold particles from the center of the PSD in the lateral plane of the synapse (normalized by PSD length) is shown as a histogram (lower panel). Shank labeling peaks ~25 nm postsynaptic of the postsynaptic membrane in the axodendritic axis and is evenly distributed in the lateral plane of the PSD.

terminus is functionally important in vivo for the targeting of Shank (but not of PSD-95) to synaptic sites. Together with the biochemical and immunostaining data, these dominant negative results support a physiological interaction between GKAP and Shank in neuronal synapses.

Shank Interaction with Cortactin

As noted above, Shank1 and Shank3 show sequence similarity to the cortactin-binding protein CortBP1. CortBP1 contains a proline-rich motif (-KPPVPPKP-) that mediates binding to the SH3 domain of cortactin (Du et al., 1998). We noted an identical sequence in the proline-rich region of Shank3 (Figure 2, residues 1410–1417) that conforms to the cortactin SH3-binding consensus +PPψXKP determined by phage-displayed peptide library screening (+, ψ, and X signify basic, aliphatic, or "any" residue, respectively; Sparks et al., 1996). Shank1 did not contain a sequence exactly matching this motif (the closest was -KPPLPPLP-, residues 1872–1879). To examine whether Shank3 can interact with cortactin, we performed pulldown assays with GST fusions of various Shank3 domains. Two constructs of Shank3 that contained the -KPPVPPKP- motif were able to bind cortactin expressed in HEK293 cells, while GST alone or fusions to other Shank domains could not (Figure 7B, upper blot). In the reverse direction, a GST fusion of full-length cortactin pulled down Shank3 (residues 1379–1740), while a GST fusion of cortactin with a specific SH3 domain deletion (cortactinΔSH3) was unable to do so (Figure 7B, lower blot). As further evidence for this interaction, full-length Shank3 was cotransfected with cortactin or cortactinΔSH3 into HEK cells. Antibodies to Shank were able to coimmunoprecipitate cortactin but not cortactinΔSH3 (Figure 7C). Preimmune serum was unable to immunoprecipitate either protein. Thus, Shank3 can bind to cortactin in vitro and in heterologous cells, and the mode of binding is similar to the CortBP1–cortactin interaction (Du et al., 1998).

In the brain, cortactin is enriched in the PSD-I fraction (which has been extracted with Triton X-100), but not in PSD-III (extracted with Triton X-100 and sarkosyl; Figure 6A). Therefore, cortactin may be weakly associated with the PSD, but unlike the Shank/GKAP/PSD-95 complex, cortactin does not behave as a core component of the PSD. We were unable to coimmunoprecipitate Shank and cortactin from brain extracts, but this is perhaps not surprising given the differential detergent

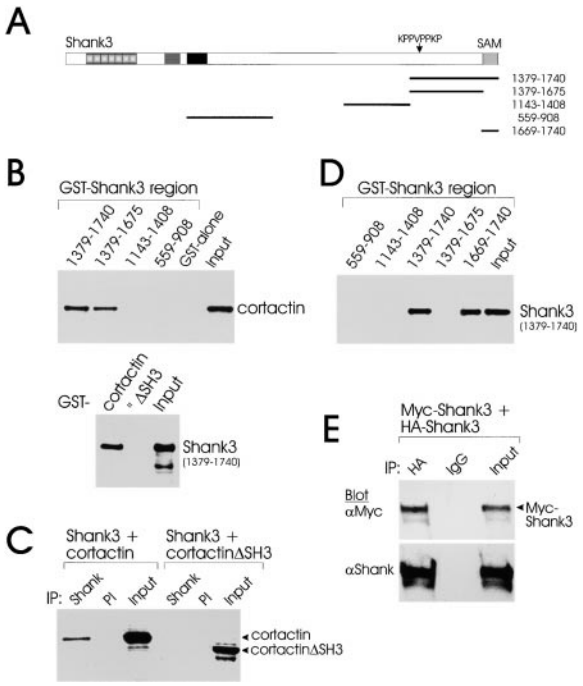

Figure 7. Cortactin Binding and Multimerization of Shank

(A) Diagram showing regions of Shank3 used in GST pulldown assays (drawn to scale). The location of the putative cortactin binding sequence (KPPVPPKP) is indicated.

(B) SH3-dependent binding of cortactin to a specific region of the Shank3 proline-rich domain. Beads charged with GST alone or with GST fusion proteins containing different regions of Shank3, full-length cortactin, or cortactin lacking its SH3 domain (cortactinΔSH3), as indicated, were incubated with extracts of HEK293 cells expressing myc-tagged full-length cortactin (upper panel) or myc–Shank3 (residues 1379–1740; lower panel). Bound proteins were immunoblotted with anti-myc antibodies. Input lane was loaded with 2.5% of extract used for pulldown.

(C) Coimmunoprecipitation of full-length Shank3 and cortactin. Extracts of HEK293 cells cotransfected with Shank3 + HA–cortactin or with Shank3 + HA–cortactinΔSH3 were immunoprecipitated with Shank antibodies or preimmune serum (PI), as indicated. Immunoprecipitates were immunoblotted for HA. Cortactin but not cortactinΔSH3 is coprecipitated by Shank antibodies. Shank3 was immunoprecipitated from both extracts by Shank antibodies, but not by preimmune serum (data not shown). Input lane was loaded with 10% of extract used for immunoprecipitation.

(D) SAM domain is sufficient for Shank self-association. Beads charged with GST fusions of Shank3 regions as indicated were incubated with extracts of HEK293 cells expressing myc–Shank3 (residues 1379–1740). Bound proteins were immunoblotted for myc. GST fusions containing the SAM domain were able to pull down myc–Shank3 (residues 1379–1740). Input lane was loaded with 2.5% of extract used for pulldown.

(E) Oligomerization of full-length Shank3 in heterologous cells. Extracts of HEK293 cells cotransfected with full-length myc–Shank3 and HA–Shank3 were immunoprecipitated using HA antibodies or nonimmune IgG and the precipitates immunoblotted for myc and Shank. HA antibodies precipitated myc–Shank3, implying self-association of Shank. Input lane was loaded with 10% of extract used for immunoprecipitation.

solubility of cortactin and Shank. Taken together, these biochemical results do not support a stable association of Shank and cortactin in vivo, but they are consistent with a regulated or low-affinity interaction between cortactin and Shank. To explore this further, we examined the subcellular distribution of cortactin in cultured hippocampal neurons (Figure 8B). In developing neurons prior to synapse formation, cortactin and Shank are colocalized in growth cones of neuritic processes (Figure 8Ba), as has been shown previously for cortactin and CortBP1 (Du et al., 1998). In more mature neurons (2 weeks in vitro), the immunostaining pattern of cortactin was densely punctate but more widespread than that of Shank (Figure 8Bb). Using a computer algorithm to quantitate the extent of area colocalization of immunofluorescent signals (see the Experimental Procedures), we found that a small fraction (6.3% $\pm$ 0.6%) of cortactin immunolabeling overlapped spatially with Shank (Figure 8Bd). Since Shank immunoreactivity is specifically clustered at synapses (see Figure 5), this minor punctate colocalization of cortactin and Shank presumably occurs at synapses (arrowheads in Figure 8Bb). Interestingly, after a 10 min stimulation of neurons with glutamate, cortactin redistributed to a more synaptic pattern, such that 25% $\pm$ 2.2% of cortactin immunolabeling colocalized with Shank ($p < 10^{-4}$) (Figures 8Bc and 8Bd). Since the algorithm used to determine this percentage does not take into account the intensity of immunostaining, and the brightest cortactin puncta colocalize with Shank, the actual mass of cortactin colocalizing with Shank is probably underestimated. The majority of Shank-immunoreactive puncta colocalize with cortactin in glutamate-stimulated neurons (see Figure 8Bc). The colocalization data in primary neuron culture are consistent with an in vivo interaction of cortactin and Shank in growth cones and in a subset of synapses. Perhaps more interestingly, they suggest that cortactin may undergo an activity-dependent redistribution into synapses. Whether this redistribution involves a regulated interaction with Shank remains to be determined.

Multimerization of Shank

Several well-characterized scaffold proteins of the PSD show the capacity for homo- or heteromultimerization, including PSD-95 and chapsyn-110/PSD-93 (Kim et al., 1996; Hsueh et al., 1997), the Homer family of proteins (Xiao et al., 1998), and GRIP/ABP (Srivastava et al., 1998). We wondered whether Shank proteins also multimerize, perhaps via the SAM domain—a domain known to mediate oligomerization (see Thanos et al., 1999, and references therein). To examine this issue, we tested whether GST fusions of various regions of Shank3 could pull down a Shank3 fragment (residues 1379–1740) containing the SAM domain from extracts of transfected HEK293 cells. GST fusions of the C-terminal region of Shank3 (residues 1379–1740) or of the SAM domain alone (residues 1669–1740) were able to bind Shank3 (residues 1379–1740), while GST fusions of three other regions of Shank could not (Figure 7D). Thus, regions of Shank3 containing the SAM domain are able to associate in vitro. In addition, when myc epitope–tagged full-length Shank3 was cotransfected with HA-tagged full-length Shank3 in HEK cells, anti-HA antibodies (but not nonimmune IgG) were able to coprecipitate myc–Shank3 with HA–Shank3 (Figure 7E). Anti-HA antibodies did not precipitate myc–Shank3 in the absence of HA–Shank3 (data not shown). Collectively, these results imply that full-length Shank protein can multimerize and

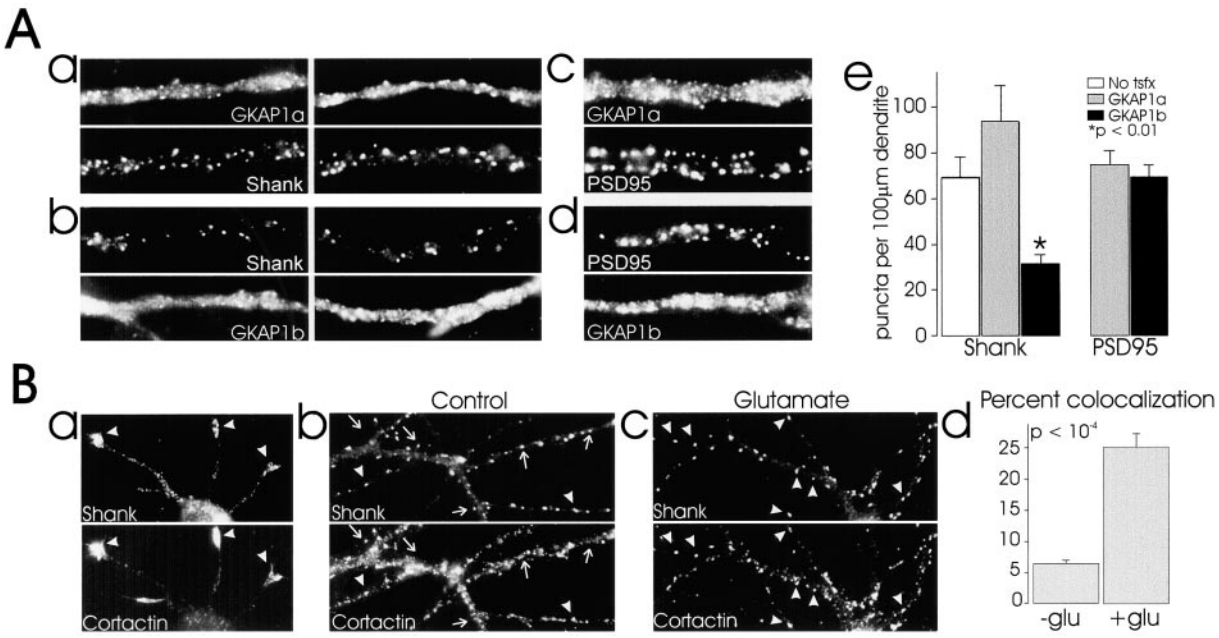

Figure 8. The Importance of GKAP Interaction on the Synaptic Localization of Shank, and Glutamate-Induced Colocalization of Cortactin and Shank in Cultured Neurons

(A) The importance of GKAP–Shank interaction for synaptic clustering of Shank in neurons.

(Aa) Two examples of neurons transfected with GKAP1a and double labeled for GKAP (upper panel of each pair) showing high levels of GKAP staining, and for Shank (lower panels), showing punctate synaptic Shank staining on dendrites that is similar to untransfected neurons (compare with Figure 5).

(Ab) Two examples of GKAP1b-transfected neurons, showing high levels of GKAP staining (lower panels) and decreased number of Shank immunoreactive clusters on dendrites (upper panels).

(Ac) GKAP1a-transfected neuron double labeled for GKAP/PSD-95, as indicated.

(Ad) GKAP1b-transfected neuron doubled labeled for GKAP/PSD-95, as indicated. The density of PSD-95 synaptic clusters was unaffected by overexpression of either GKAP1a (Ac) or GKAP1b (Ad).

(Ae) Quantitation of data shown representatively in (Aa)–(Ad). The number of clusters of Shank and PSD-95 per 100 μm dendrite in neurons transfected with GKAP1a (gray bars) or GKAP1b (black), or in untransfected neurons (white) were counted using Metamorph software by a blind observer (see the Experimental Procedures). Bars show mean $\pm$ SEM; * indicates $p < 0.01$ compared with either GKAP1a-transfected or untransfected neurons. In contrast, PSD-95 and synaptophysin clustering are not significantly different in GKAP1a- versus GKAP1b-transfected neurons ($p = 0.52$ and $p = 0.35$, respectively). See the Experimental Procedures for details.

(B) Colocalization of cortactin and Shank in cultured neurons.

(Ba) Cortactin and Shank colocalize in growth cones of developing neurons (arrowheads).

(Bb) Mature neuron double labeled for cortactin and Shank. Only a small fraction of puncta colocalize along dendrites (examples indicated by arrowheads); most labeling does not overlap (arrows).

(Bc) After treatment with glutamate (100 μm for 10 min), there is a marked increase in colocalization of Shank and cortactin (arrowheads), such that most Shank immunoreactive puncta are also cortactin positive.

(Bd) Quantitation of data shown representatively in (Bb) and (Bc). The percent (pixel) area of cortactin labeling that overlaps with Shank labeling was determined using Metamorph colocalization software and plotted as mean $\pm$ SEM.

that the Shank SAM domain is sufficient to mediate this self-association.

Discussion

GKAP–Shank Interaction in Synapses

We report here a novel family of proteins (Shank) that is specifically localized in excitatory synapses and highly enriched in the PSD. Shank interacts directly with GKAP and appears to be a major component of the PSD-95/GKAP protein complex that is associated with NMDA receptors at postsynaptic sites. The multiple genes in the Shank family, and their complex alternative splicing, give rise to a remarkable heterogeneity of Shank polypeptides. Since a C-terminal (-QTRL) sequence shared by all four GKAP/SAPAP genes can bind to the conserved PDZ domains of Shank1–3, we predict that a wide variety of GKAP and Shank proteins can interact with each other. Different combinations of the various GKAPs and Shanks could generate a heterogeneity of associations in vivo. An additional level of complexity is represented by a C-terminal splice variant of GKAP (GKAP1b) that does not bind Shank. GKAP1b transfection into neurons inhibits Shank recruitment to synapses, suggesting that the targeting of Shank to the PSD can be regulated by alternative splicing of GKAP. Although GKAP1b overexpression interferes with the synaptic localization of Shank, it does not inhibit the synaptic localization of PSD-95. We conclude that GKAP is a critical determinant of Shank's synaptic localization, but Shank is not required for PSD-95/GKAP targeting to synapses. Thus, Shank recruitment to synapses can be considered downstream of or secondary to PSD-95/GKAP synaptic localization.

Multidomain Organization and Multiple Protein Interactions of Shank

A key to understanding Shank function lies in the structural organization of this family of proteins. The Shank sequence shows an absence of known enzymatic/catalytic domains but an abundance of motifs that are likely involved in binding to other proteins. These include ankyrin repeats, the SH3 domain, the PDZ domain, proline-rich motifs, and the SAM domain (see diagram in Figure 1A). The role of the seven ankyrin repeats in Shank is unknown, but such repeats are implicated as protein interaction domains in other proteins (Bork, 1993; Jacobs and Harrison, 1998). C-terminal to the ankyrin repeats, Shank contains another well-known protein-binding module, the SH3 domain. The presumptive ligands of the Shank SH3 domain also remain to be identified.

Adjacent to the SH3 domain of Shank is the PDZ domain, which we have determined mediates Shank binding to the C terminus of GKAP. The PDZ domain of Shank has a distinctive binding specificity, preferring the hydrophobic residue leucine over valine at the very C terminus of interacting proteins. This contrasts with the better known PDZ domains of PSD-95, which prefer valine at the 0 position. In addition, the Shank PDZ prefers positive charge over negative charge at the -1 position, whereas the best characterized ligands for the first two PDZ domains of PSD-95 (NMDA receptor NR2 subunits, and Shaker-type potassium channels) have a negatively charged aspartate in this position. A neutral amino acid may also be acceptable at -1 (see Tu et al., 1999). Based on sequence comparisons with PDZ domains of known binding specificity (Songyang et al., 1997) and the crystal structure of a PDZ–peptide complex (Doyle et al., 1996), we hypothesize that the presence of isoleucine (residue 670 in Shank1a or 649 in Shank3a) at αB8 might contribute to Shank's preference for leucine over valine at the the 0 position. The negatively charged glutamate (residue 631 in Shank1a or 610 in Shank3a) at βC5 (instead of lysine in PDZ1/2 of PSD-95) may contribute to Shank PDZ preference for a positive charge at the -1 position.

The extensive region lying between the PDZ domain and the SAM domain of Shank is rich in proline (22% in Shank1, 16% in Shank3) and serine residues (16% in Shank1, 12% in Shank3). Proline-rich motifs often mediate protein–protein association, serving as binding sites for modules such as SH3, EVH, and WW domains (Bedford et al., 1997; Nguyen et al., 1998). We have identified two ligands for the proline-rich region of Shank: cortactin, which binds the -KPPVPPKP- motif with its SH3 domain, and Homer, which binds to the -PPXXF- motif (-PPLEF- in Shank1, -PPEEF- in Shank3), with its EVH domain (Tu et al., 1998; discussed in detail in the accompanying paper, Tu et al., 1999).

The C terminus of Shank is occupied by a SAM domain, which is found in a variety of signal transducing proteins, including Eph receptor tyrosine kinases. Interestingly, the SAM domain is found at the C terminus of all Eph receptors, the same position it occupies in the Shank polypeptides. Previous studies suggest that SAM domains can form homo- and/or heterooligomers (Jousset et al., 1997; Peterson et al., 1997; Thanos et al., 1999). The crystal structure of the SAM domain from the EphB2 receptor has revealed two distinct interfaces for SAM–SAM interaction that would allow formation of an extended polymer of SAM domains (Thanos et al., 1999). We show here that full-length Shank can multimerize and that the SAM domain of Shank is sufficient for self-association, suggesting that Shank may exist as an oligomer linked via its C-terminal SAM. In the context of the PSD, oligomerization of Shank SAM domains may be significant for cross-linking multiple sets of protein complexes, such as the NMDA receptor/PSD-95/GKAP complex and the mGluR/Homer complex (Tu et al., 1999). It will be interesting to examine if SAM-mediated self-association of Shank proteins is regulated in synapses, because the degree of oligomerization of Shank could influence the structural organization of the PSD.

Interaction with Cortactin and Regulation of Actin Cytoskeleton

Neurons, like other cells, undergo rearrangements of the cortical actin cytoskeleton in response to extracellular signals. The actin cytoskeleton of the dendritic spine is particularly dynamic (Fischer et al., 1998), and activity-dependent reorganization of the postsynaptic cytoskeleton may play a role in the plasticity of excitatory synapses. Little is understood, however, about the mechanisms that might couple synaptic stimulation to cytoskeletal changes in dendritic spines. Here, we have shown that Shank binds to cortactin, a protein implicated in signaling to the actin cytoskeleton. Originally identified as a substrate of Src tyrosine kinase, cortactin is an F-actin-binding protein enriched in cell–matrix contact sites, membrane ruffles and lammelipodia of cultured cells, and in growth cones of neurons (Wu and Parsons, 1993; Du et al., 1998). The translocation of cortactin to the cell periphery is stimulated by the small GTPase Rac1 (Weed et al., 1998), and its F-actin cross-linking activity is inhibited by Src tyrosine phosphorylation (Huang et al., 1997). Thus, a large body of evidence implicates cortactin in regulation of the actin cytoskeleton in dynamic regions of the cell periphery. Our study suggests that cortactin may also play a role in neuronal synapses, based on the following findings: biochemically, cortactin is loosely associated with the PSD, and immunocytochemically, it colocalizes with Shank in a subset of synapses. Most interestingly, we have demonstrated a significant redistribution of cortactin to synaptic sites in response to glutamate stimulation. The glutamate-induced synaptic localization of cortactin is reminiscent of cortactin recruitment to the cortical cytoskeleton by growth factor stimulation of nonneural cells (Weed et al., 1998). Their coexistence in growth cones provides further suggestion that Shank and cortactin may function at sites of active cytoskeletal remodeling in neurons. In mature synapses, we speculate that a regulated Shank–cortactin interaction may be a mechanism for linking NMDA receptor activation to the control of the postsynaptic actin cytoskeleton.

Shanks are highly related to CortBP1, a protein isolated by yeast two-hybrid screening with the SH3 domain of cortactin (Du et al., 1998). CortBP1 has been shown to colocalize with cortactin in membrane ruffles of cultured cells and in growth cones of cultured neurons (Du et al., 1998), analogous to our colocalization of Shank and cortactin in growth cones and synapses.

Based on their similarity in primary structure and cell biological properties, it seems reasonable to consider CortBP1 and Shanks as members of the same family of proteins.

Shank, a Higher Order Scaffold Protein for the PSD

What then is the function of Shank? Our cloning and characterization of Shank has revealed its large size, its multidomain structure supporting diverse protein interactions (including self-association), its specific localization in the PSD of excitatory synapses, and its association with the PSD-95/GKAP complex. In the accompanying paper, we report that Shank also binds to Homer, the anchoring protein for mGluR1/5 (Tu et al., 1999). All these features point to Shank being a new scaffold protein of the postsynapse. If PSD-95 can be considered a scaffold protein of the PSD operating close to the postsynaptic membrane (a membrane-proximal scaffold that binds directly to NMDA receptors), we propose that Shank plays the role of key scaffold protein in the deeper levels of the PSD (several proteins removed from the membrane receptors). Indeed, the immunogold quantitation suggests that Shank (peaking at ~25 nm inside of the postsynaptic membrane) is localized in a deeper part of the PSD than are PSD-95 or NMDA receptors (J. V. and R. J. W., unpublished data). Being further from the membrane (in a topological as well as a physical sense), Shank is in the appropriate position to connect together the different glutamate receptors and their respective protein complexes and to serve as an interface between these signaling complexes and the actin cytoskeleton of the dendritic spine.

Experimental Procedures

Yeast Two-Hybrid Screen and Analysis of GKAP–Shank Interaction

Yeast two-hybrid screening and assays were performed as described previously (Bartel et al., 1993; Niethammer and Sheng, 1998) using the L40 yeast strain harboring HIS3 and β-gal as reporter genes. GKAP1a residues 591–666 were subcloned into pBHA (LexA fusion vector) and used to screen ~1.5 × 10^6 clones from rat and human cDNA libraries constructed in pGAD10 (GAL4 activation domain vector, Clontech). For analysis of specificity and binding domains, desired cDNA segments were amplified by PCR with specific primers and subcloned into pBHA or pGAD10. Two-hybrid constructs of Kv1.4 and PSD-95 have been described (Kim et al., 1995). Shank1(SH3–PDZ) contains residues 469–691, and Shank1(PDZ) contains residues 684–691 of Shank1a. Mutations of GKAP C-terminal residues were generated by PCR of GKAP1a (residues 591–666) using antisense primers containing specific nucleotide substitutions.

Antibodies

Shank antibodies were raised in rabbits against a GST fusion of Shank1a residues 469–691 and affinity purified using a thioredoxin fusion of same region (these are termed Shank 56/8 antibodies). In some experiments, the IgG fraction purified by protein A–sepharose was used (these are termed Shank 56/e antibodies). Identical bands were seen on rat brain immunoblots using both antibody preparations, and preincubation with a thioredoxin fusion of Shank1 (residues 469–591) abolished the signal of both antibodies (data not shown). In addition, an independent peptide antibody raised against a nonoverlapping region of Shank1 (residues 422–440) detected identical bands on rat brain immunoblots (E. K., S. N., and M. S., unpublished data). The following antibodies have been described: anti-GKAP N1564 and C9589 (Kim et al., 1997; Naisbitt et al., 1997); guinea pig anti-PSD-95 (Kim et al., 1995); anti-cortactin mouse monoclonal 4F11, a gift from Tom Parsons (Kanner et al., 1990). Anti-PSD-95 family mouse monoclonal antibodies (K28/86, Upstate Biotechnology) detect PSD-95, chapsyn-110/PSD-93, and SAP97 on immunoblots. Other antibodies are described under the assays in which they were used.

Shank Cloning and Plasmid Constructs

Full-length Shank1 and Shank3 cDNAs were obtained by standard hybridization screening of λZAP II rat cortical and hippocampal cDNA libraries (Stratagene) using digoxigenin-labeled DNA probes from fragments initially isolated in the yeast two-hybrid screen. Full-length Shank1a cDNA constructs in GWI-CMV (British Biotechnology) were made by ligating restriction digested fragments from two-hybrid prey and λZAP II clones as follows: HindIII (nt 0, site introduced by short PCR)–BamHI (nt 1099) from clone 5–1; BamHI (nt 1099)–EcoRI (nt 2079) from clone r8/6; EcoRI (nt 2079)–BsawI (nt 3079) from prey clone r19; BsawI (nt 3079)–NotI (nt 3514) from r19/18; NotI (nt 3514)–AvrII (nt 4279) from clone 3–10; and AvrII (nt 4340)–SalI (nt 7090) from clone 1–3–1 (including 3′UTR). For experiments in COS7 cells, we used a Shank1a construct extending to clone 3–10 (diverging at nt 4759, residue 1509 of Shank1a, and thus omitting the SAM domain) because full-length Shank1a expressed poorly. For Shank3 expression constructs, see Tu et al. (1999).

Transfection and Clustering in Heterologous Cells

COS-7 cells were transfected with Lipofectamine (GIBCO-BRL) on polylysine-coated coverslips (for clustering experiments) or in 100 mm tissue culture dishes (for immunoprecipitation experiments). Cells were fixed and permeabilized as described 24 hr after transfection (Kim et al., 1996; for concentrations of primary and secondary antibodies, see Neuron Culture, Immunocytochemistry and Immunoelectron Microscopy below).

Pulldown, Immunoprecipitation, and Biochemical Fractionation

For pulldown experiments, whole brain homogenate was extracted in 1% SDS and quenched in Tx-100 as described (Müller et al., 1996; Kim et al., 1997), except that quenching buffer contained (in mM): 130 KCl, 10 NaCl, 2 $MgCl_2$, 3 EGTA, 50 HEPES (pH 7.4), and 1% Tx-100. After 1 hr centrifugation at 100,000 × g, 120 μg extract was incubated with glutathione sepharose 4B (Amersham Pharmacia Biotech) coupled to 6 μg GST or GST fusion (approximately 3 μl bed volume) for 2 hr at 4°C, followed by four washes in quenching buffer. Pulldowns and immunoprecipitations from transfected HEK293 cell extracts were performed as described in the accompanying paper (Tu et al., 1999). For immunoprecipitation from COS7 cell extracts, cells were washed and pelleted followed by resuspension in (in mM): 50 Tris (pH 7.4), 75 NaCl, 2.5 EGTA, 2.5 EDTA, 1% SDS, followed by 4-fold dilution in 1% Tx-100, 50 Tris (pH 7.4), 150 NaCl, 2.5 EGTA, 2.5 EDTA plus protease inhibitors and 1 hr 16,000 × g centrifugation. Supernatants were incubated with 2 μg of control nonimmune IgG, Shank 56/e, or a 1:1 mixture of GKAP N1564 and C9589 antibodies. Extracts of forebrain synaptosomes for immunoprecipitation were prepared using either SDS (more efficient for GKAP coimmunoprecipitation with Shank) or DOC (more efficient for Shank coimmunoprecipitation with GKAP). Extraction of forebrain P2 in 1% DOC was performed as described (Dunah et al., 1998) followed by dialysis overnight into 0.1% Tx-100, 50 mM Tris (pH 7.4). Concurrently, 5 μg each antibody was preincubated overnight with 10 μl protein A–sepharose. After clearing at 100,000 × g for 1 hr, dialyzed extract (50 μg protein) was incubated with antibody–protein A in 100 μl 0.1% Tx-100, 50 mM Tris, (pH 7.4) for 2 hr at 4°C. Precipitates were washed four times with 1 ml of incubation buffer. For antigen competition controls, TRX–gk2.1 (see Kim et al., 1997) or TRX-GKAP1a(C-term) at 100 μg/ml concentration were present during all antibody incubation steps. For SDS extraction, the 1% Tx-100-insoluble pellet from P2 was solubilized in 1% SDS plus 5 mM ATP, 0.05% β-mercaptoethanol, followed by 4-fold dilution in 1% Tx-100 quenching buffer plus 5 mM ATP, 0.05% β-mercaptoethanol. After centrifugation at 100,000 × g for 1 hr, soluble extract (300 μg protein) was incubated with 2.5 μg of control nonimmune IgG, Shank 56/e, or GKAP N1564 antibodies. After 2 hr incubation at 4°C, 10 μl protein A–sepharose beads was added for 2 hr. Pellets were washed four times in Tx-100 quenching buffer. Detergent-extracted PSDI-III fractions were prepared as previously described (Cho et al., 1992). Immunoblotting was developed with enhanced chemiluminescence reagents (ECL, Amersham).

Neuron Culture, Immunocytochemistry, and Immunoelectron Microscopy

Low-density hippocampal neuronal cultures were prepared from E18 rats as described (Goslin and Banker, 1991). After 2–3 weeks in culture, neurons were fixed in methanol for 10 min at −20°C and incubated overnight at 4°C with primary antibodies at the following dilutions: Shank 56/e, 0.5 μg/ml; Synaptophysin SVP38 monoclonal (SIGMA), 1:1000; GAD monoclonal (Boehringer Mannheim), 1 μg/ml; PSD-95 guinea pig serum, 1:1000; GKAP N1564 or GKAP C9589, 1 μg/ml; NMDAR1 monoclonal 54.1 (PharMingen), 2.5 μg/ml. Cy3- and FITC-conjugated secondary antibodies (Jackson Immunoresearch) were used at dilutions of 1:500 and 1:100, respectively. Immunofluorescence was visualized with a Zeiss Axioskop microscope, and digital images were prepared for publication with Adobe Photoshop. Postembedding immunogold electron microscopy was performed and quantified as described (Phend et al., 1995; Naisbitt et al., 1997) using Shank antibody 56/e at 1 μg/ml. Only sparse scattered immunogold labeling was seen in the absence of primary antibody (data not shown).

Neuron Culture Transfection and Quantification of Immunolabeling

For GKAP transfections, neuron cultures were prepared from trypsin-dissociated E18–E19 hippocampi and plated on polylysine-coated coverslips in MEM containing 10% FCS, 25 μg/ml insulin, 100 μg/ml transferrin, 1 mM pyruvate, and 0.6% glucose. Transfections of GW1-GKAP1a or GW1-GKAP1b were performed at 3 days in vitro using the calcium phosphate method as described (Xia et al., 1996). Neurons were fixed and processed for double-labeled immunostaining as described above 7–10 days after transfection. GKAP1a- or GKAP1b-transfected neurons were easily recognized by their much higher levels of GKAP staining. GKAP1a-transfected neurons were double labeled for Shank ($n = 7$) or PSD-95 ($n = 13$) or synaptophysin ($n = 7$) in addition to GKAP. Similarly, GKAP1b-transfected neurons were double labeled for Shank ($n = 13$) or PSD-95 ($n = 23$) or synaptophysin ($n = 15$). Images of transfected neurons and untransfected controls ($n = 7$) were acquired using an interline cooled CCD camera (Princeton Instruments) and analyzed by a blind observer using Metamorph software (Universal Imaging). For each neuron, immunolabeled puncta having intensity above a blind user–defined threshold were counted by Metamorph software and normalized for dendritic length. An unpaired, two-tailed Student's t test on these sample arrays (having unequal variance by ANOVA) yielded $p < 0.01$ for Shank-labeled GKAP1b-transfected neurons when compared against either GKAP1a-transfected or untransfected cells ($p = 0.008$ or $p = 0.006$, respectively). For cortactin redistribution experiments, low-density hippocampal neurons were prepared as described (Goslin and Banker, 1991). After 2 weeks in culture, glutamate (100 μM) was added directly to the medium for 10 min. Neurons were then fixed in methanol at 20°C and immunolabeled as described above. Images were acquired as above, using constant camera exposure times within each experiment. Neurons were randomly chosen from treated and untreated cultures and subjected to a user-defined intensity threshold (kept constant within each experiment). Using this threshold, a colocalization index was obtained using Metamorph colocalization software, yielding the percent area (pixels) of cortactin signal that overlaps with Shank signal. Statistical significance was determined as above.

Acknowledgments

We thank Fu-Chia Yang for experimental help, J. Thomas Parsons (University of Virginia) for cortactin cDNA and antibodies, and Pann-Ghill Suh for Shank monoclonal antibodies. M. S. is an Assistant Investigator of the Howard Hughes Medical Institute. C. S. is a Harvard-Armenise Foundation Fellow (Department of Biological and Technical Reseach, Hospital San Raffaele, Scientific Institute, San Raffaele, Italy). This work was supported by the National Institutes of Health grants NS35050 (M. S.) and NS29879 (R. J. W.), the National Institute on Drug Abuse grants DA103009 and DA11742, the National Institute of Mental Health grant K02MH01152 (P. W.), and Korea Science and Engineering Foundation grant 981-0713-099-2 (E. K.).

Received March 1, 1999; revised June 24, 1999.

References

Allison, D.W., Gelfand, V.I., Spector, I., and Craig, A.M. (1998). Role of actin in anchoring postsynaptic receptors in cultured hippocampal neurons: differential attachment of NMDA versus AMPA receptors. J. Neurosci. *18*, 2423–2436.

Bartel, P.L., Chien, C.T., Sternglanz, R., and Fields, S. (1993). Using the 2-hybrid system to detect protein-protein interactions in cellular interactions in development: a practical approach, D.A. Hartley, ed. (Oxford: Oxford University Press).

Bedford, M.T., Chan, D.C., and Leder, P. (1997). FBP WW domains and the Abl SH3 domain bind to a specific class of proline-rich ligands. EMBO J. *16*, 2376–2383.

Bork, P. (1993). Hundreds of ankyrin-like repeats in functionally diverse proteins: mobile modules that cross phyla horizontally? Proteins *17*, 363–374.

Brakeman, P.R., Lanahan, A.A., O'Brien, R., Roche, K., Barnes, C.A., Huganir, R.L., and Worley, P.F. (1997). Homer, a protein that selectively binds metabotropic glutamate receptors. Nature *386*, 284–288.

Cho, K.-O., Hunt, C.A., and Kennedy, M.B. (1992). The rat brain postsynaptic density fraction contains a homolog of the Drosophila discs-large tumor suppressor protein. Neuron *9*, 929–942.

Cohen, R.S., Blomberg, F., Berzins, K., and Siekevitz, P. (1977). The structure of postsynaptic densities isolated from dog cerebral cortex. I. Overall morphology and protein composition. J. Cell Biol. *74*, 181–203.

Cotman, C.W., Banker, G., Churchill, L., and Taylor, D. (1974). Isolation of postsynaptic densities from rat brain. J. Cell Biol. *63*, 441–455.

Craven, S., and Bredt, D. (1998). PDZ proteins organize synaptic signaling pathways. Cell *15*, 495–498.

Dong, H., O'Brien, R.J., Fung, E.T., Lanahan, A.A., Worley, P.F., and Huganir, R.L. (1997). GRIP: a synaptic PDZ domain-containing protein that interacts with AMPA receptors. Nature *386*, 279–284.

Doyle, D.A., Lee, A., Lewis, J., Kim, E., Sheng, M., and MacKinnon, R. (1996). Crystal structures of a complexed and peptide-free membrane protein-binding domain: molecular basis of peptide recognition by PDZ. Cell *85*, 1067–1076.

Du, Y., Weed, S.A., Xiong, W.-C., Marshall, T.D., and Parsons, J.T. (1998). Identification of a novel cortactin SH3 domain-binding protein and its localization to growth cones of cultured neurons. Mol. Cell. Biol. *18*, 5838–5851.

Dunah, A., Luo, J., Wang, Y., Yasuda, R., and Wolfe, B. (1998). Subunit composition of N-methyl-D-aspartate receptors in the central nervous system that contain the NR2D subunit. Mol. Pharmacol. *53*, 429–437.

Fischer, M., Kaech, S., Knutti, D., and Matus, A. (1998). Rapid actin-based plasticity in dendritic spines. Neuron *20*, 847–854.

Goslin, K., and Banker, G. (1991). Rat hippocampal neurons in low-density culture. In Culturing Nerve Cells, G. Banker and K. Goslin, eds. (Cambridge, MA: The MIT Press).

Hsueh, Y.-P., Kim, E., and Sheng, M. (1997). Disulfide-linked head-to-head multimerization in the mechanism of ion channel clustering by PSD-95. Neuron *18*, 803–814.

Huang, C., Ni, Y., Wang, T., Gao, Y., Haudenschild, C.C., and Zhan, X. (1997). Down-regulation of the filamentous actin cross-linking activity of cortactin by Src-mediated tyrosine phosphorylation. J. Biol. Chem. *272*, 13911–13915.

Jacobs, M.D., and Harrison, S.C. (1998). Structure of an IκBα/NF-κB complex. Cell *95*, 749–758.

Jousset, C., Carron, C., Boureux, A., Quang, C., Oury, C., Dusanter-Fourt, I., Charon, M., Levin, J., Bernard, O., and Ghysdael, J. (1997). A domain of TEL conserved in a subset of ETS proteins defines a specific oligomerization interface essential to the mitogenic properties of the TEL-PDGFR beta oncoprotein. EMBO J. *16*, 69–82.

Kanner, S.B., Reynolds, A.B., Vines, R.R., and Parsons, J.T. (1990). Monoclonal antibodies to individual tyrosine-phosphorylated protein substrates of oncogene-encoded tyrosine kinases. Proc. Natl. Acad. Sci. USA *87*, 3328–3332.

Kato, A., Ozawa, F., Saitoh, Y., Fukazawa, Y., Sugiyama, H., and Inokuchi, K. (1998). Novel members of the Vesl/Homer family of PDZ

proteins that bind metabotropic glutamate receptors. J. Biol. Chem. *273*, 23969–23975.

Kennedy, M.B. (1997). The postsynaptic density at glutamatergic synapses. Trends Neurosci. *20*, 264–268.

Kim, E., Niethammer, M., Rothschild, A., Jan, Y.N., and Sheng, M. (1995). Clustering of shaker-type K^+ channels by interaction with a family of membrane-associated guanylate kinases. Nature *378*, 85–88.

Kim, E., Cho, K.-O., Rothschild, A., and Sheng, M. (1996). Heteromultimerization and NMDA receptor-clustering activity of chapsyn-110, a member of the PSD-95 family of proteins. Neuron *17*, 103–113.

Kim, E., Naisbitt, S., Hsueh, Y.-P., Rao, A., Rothschild, A., Craig, A.M., and Sheng, M. (1997). GKAP, a novel synaptic protein that interacts with the guanylate kinase-like domain of the PSD-95/SAP90 family of channel clustering molecules. J. Cell Biol. *136*, 669–678.

Kim, E., Niethammer, M., Rothschild, A., Jan, Y.N., and Sheng, M. (1995). Clustering of shaker-type K^+ channels by interaction with a family of membrane-associated guanylate kinases. Nature *378*, 85–88.

Kornau, H., Seeburg, P., and Kennedy, M. (1997). Interaction of ion channels and receptors with PDZ domain proteins. Curr. Opin. Neurobiol. *7*, 368–373.

Müller, B.M., Kistner, U., Veh, R.W., Cases-Langhoff, C., Becker, B., Gundelfinger, E.D., and Garner, C.C. (1995). Molecular characterization and spatial distribution of SAP97, a novel presynaptic protein homologous to SAP90 and the *Drosophila* discs-large tumor suppressor protein. J. Neurosci. *15*, 2354–2366.

Müller, B.M., Kistner, U., Kindler, S., Chung, W.J., Kuhlendahl, S., Lau, L.-F., Veh, R.W., Huganir, R.L., Gundelfinger, E.D., and Garner, C.C. (1996). SAP102, a novel postsynaptic protein that interacts with the cytoplasmic tail of the NMDA receptor subunit NR2B. Neuron *17*, 255–265.

Müller, B.M., Kistner, U., Veh, R.W., Cases-Langhoff, C., Becker, B., Gundelfinger, E.D., and Garner, C.C. (1995). Molecular characterization and spatial distribution of SAP97, a novel presynaptic protein homologous to SAP90 and the *Drosophila* discs-large tumor suppressor protein. J. Neurosci. *15*, 2354–2366.

Naisbitt, S., Kim, E., Weinberg, R.J., Rao, A., Yang, F.-C., Craig, A.M., and Sheng, M. (1997). Characterization of guanylate kinase-associated protein, a postsynaptic density protein at excitatory synapses that interacts directly with postysynaptic density-95/synapse-associated protein 90. J. Neurosci. *17*, 5687–5696.

Nguyen, J.T., Turck, C.W., Cohen, F.E., Zuckermann, R.N., Lim, W.A. (1998). Exploiting the basis of proline recognition by SH3 and WW domains: design of N-substituted inhibitors. Science *282*, 2088–2092.

Niethammer, M., and Sheng, M. (1998). Identification of ion channel-associated proteins using the yeast two-hybrid system. In Methods in Enzymology *293*, P.M. Conn, ed. (New York: Academic Press), pp. 104–122.

O'Brien, R., Lau, L., and Huganir, R. (1998). Molecular mechanisms of glutamate receptor clustering at excitatory synapses. Curr. Opin. Neurobiol. *8*, 364–369.

Peterson, A.J., Kyba, M., Bornemann, D., Morgan, K., Brock, H., and Simon, J. (1997). A domain shared by the Polycomb group proteins Scm and ph mediates heterotypic and homotypic interactions. Mol. Cell. Biol. *17*, 6683–6692.

Phend, K.D., Rustioni, A., and Weinberg, R.J. (1995). An osmium-free method of Epon embedment that preserves both ultrastructure and antigenicity for postembedding immunocytochemistry. J. Histochem. Cytochem. *43*, 283–292.

Rao, A., Kim, E., Sheng, M., and Craig, A. (1998). Heterogeneity in the molecular composition of excitatory postsynaptic sites during development of hippocampal neurons in culture. J. Neurosci. *18*, 1217–1229.

Satoh, K., Yanai, H., Senda, T., Kohu, K., Nakamura, T., Okumura, N., Matsumine, A., Kobayashi, S., Toyoshima, K., and Akiyama, T. (1997). DAP-1, a novel protein that interacts with the guanylate kinase-like domains of hDLG and PSD-95. Genes Cells *2*, 415–424.

Sheng, M. (1996). PDZs and receptor/channel clustering: rounding up the latest suspects. Neuron *17*, 575–578.

Sheng, M. (1997). Glutamate receptors put in their place. Nature *386*, 221–223.

Songyang, Z., Fanning, A.S., Fu, C., Xu, J., Marfatia, S.M., Chishti, A.H., Crompton, A., Chan, A.C., Anderson, J.M., and Cantley, L.C. (1997). Recognition of unique carboxyl-terminal motifs by distinct PDZ domains. Science *275*, 73–77.

Sparks, A., Rider, J., Hoffman, N., Fowlkes, D., Quillam, L., and Kay, B. (1996). Distinct ligand preferences of Src homology 3 domains from Src, Abl, cortactin, p53BP2, PLCγ, Crk, and Grb2. Proc. Natl. Acad. Sci. USA *93*, 1540–1544.

Srivastava, S., Osten, P., Vilim, F., Khatri, L., Inman, G., States, B., Daly, C., DeSouza, S., Abagyan, R., Valtschanoff, J., Weinberg, R., and Ziff, E. (1998). Novel anchorage of GluR2/3 to the postsynaptic density by the AMPA receptor-binding protein ABP. Neuron *21*, 581–591.

Takeuchi, M., Hata, Y., Hirao, K., Toyoda, A., Irie, M., and Takai, Y. (1997). SAPAPs. a family of PSD-95/SAP90-associated proteins localized at postsynaptic density. J. Biol. Chem. *272*, 11943–11951.

Thanos, C.D., Goodwill, K.E., and Bowie, J.U. (1999). Oligomeric structure of the human EphB2 receptor SAM domain. Science *283*, 833–836.

Tu, J.C., Xiao, B., Yuan, J.P., Lanahan, A.A., Leoffert, K., Li, M., Linden, D.J., and Worley, P.F. (1998). Homer binds a novel proline-rich motif and links group 1 metabotropic glutamate receptors with IP3 receptors. Neuron *21*, 717–726.

Tu, J.C., Xiao, B., Naisbitt, S., Yuan, J.P., Petralia, R.S., Brakeman, P., Doan, A., Aakalu, V.K., Lanahan, A.A., Sheng, M., and Worley, P.F. (1999). Coupling of mGluR/Homer and PSD-95 complexes by the Shank family of postsynaptic density proteins. Neuron *23*, this issue, 583–592.

Weed, S.A., Du, Y., and Parsons, J.T. (1998). Translocation of cortactin to the cell periphery is mediated by the small GTPase Rac1. J. Cell Sci. *111*, 2433–2443.

Wenthold, R.J., Yokotani, N., Doi, K., and Wada, K. (1992). Immunochemical characterization of the non-NMDA glutamate receptor using subunit-specific antibodies. Evidence for a hetero-oligomeric structure in rat brain. J. Biol. Chem. *267*, 501–507.

Wenthold, R.J., Petralia, R.S., Blahos, J.I., and Niedzielski, A.S. (1996). Evidence for multiple AMPA receptor complexes in hippocampal CA1/CA2 neurons. J. Neurosci. *16*, 1982–1989.

Wu, H., and Parsons, J.T. (1993). Cortactin, and 80/85-kilodalton pp60src substrate, is a filamentous actin-binding protein enriched in the cell cortex. J. Cell Biol. *120*, 1417–1426.

Wyszynski, M., Kim, E., Yang, F.-C., and Sheng, M. (1998). Biochemical and immunocytochemical characterization of GRIP, a putative AMPA receptor anchoring protein, in rat brain. Neuropharmacology *37*, 1335–1334.

Xia, Z., Dudek, H., Miranti, C., and Greenberg, M. (1996). Calcium influx via the NMDA receptor induces immediate early gene transcription by a MAP kinase/ERK-dependent mechanism. J. Neurosci. *16*, 5425–5436.

Xia, J., Zhang, X., Staudinger, J., and Huganir, R.L. (1999). Clustering of AMPA receptors by the synaptic PDZ domain-containing protein PICK1. Neuron *22*, 179–187.

Xiao, B., Tu, J.C., Petralia, R.S., Yuan, J.P., Doan, A., Breder, C.D., Ruggiero, A., Lanahan, A.A., Wenthold, R.J., and Worley, P.F. (1998). Homer regulates the association of group 1 metabotropic glutamate receptors with multivalent complexes of homer-related, synaptic proteins. Neuron *21*, 707–716.

Ziff, E.B. (1997). Enlightening the postsynaptic density. Neuron *19*, 1163–1174.

GenBank Accession Numbers

Shank1a and Shank3a sequences have been deposited in GenBank under accession numbers AF131951 and AF133301, respectively.